Paper No.
C2024-20668

AMPP ANNUAL CONFERENCE + EXPO
MARCH 3-7, 2024 | NEW ORLEANS, LOUISIANA

Predicting Corrosion of Successive Feeds in Distilling Units – An Experimental Approach

Gheorghe Bota, Ishan Patel, Peng Jin, David Young
Ohio University
Institute for Corrosion and Multiphase Technology
342 West State St.
Athens, OH 45701
USA

ABSTRACT

Cheap heavy crudes become attractive for oil refineries to increase their benefit margins but the corrosivity of heavy crudes compels the refinery engineers to blend them with the more expensive light sweet crudes. Crude oil blends with complex composition including organo-sulfur compounds, fatty acids, nitrogen and chlorine compounds become corrosive when processed at high temperatures due to these reactive species. Therefore, maintaining corrosion control is a constant effort in oil refineries, and it involves the use of dedicated corrosion models combined with specific experimental lab procedures and methods. This work is presenting the practical application of a lab testing procedure used for predicting the high temperature corrosivity of different crude fractions that were run successively for different time periods in a specific “flow-through” apparatus. The testing procedure consists of two distinct phases performed in the same apparatus, at the same temperature, and for different time durations. During the first phase of the test, scales are formed using a distilling fraction on metal samples and further, in the second test phase, these preformed scales on samples are exposed without interruption to a different distilling fraction. Thus, the two successive test phases, each using a different distilling fraction, are associated with the “changing feeds” in the distilling tower. Corrosive effects are evaluated by sample weight loss measured in successive fraction tests and in separate tests performed with each of the selected fractions. Experimental results are compared to predictions of a corrosion model for sulfidation and naphthenic acid corrosion.

Keywords: sulfur, hydrocarbons, naphthenic (NAP) acid, corrosives in refining process, laboratory methods.

INTRODUCTION

Crude oil with its processing final products remains one of the main sources of energy in the world. The 2023 forecasts for oil global supplies were of 100.9 mb/b, an estimation that was falling short of oil global demand which was of 102 mb/d for the same year.[1,2] The high crude oil

demand constrained the refining industry to process oils of different quality, to optimize the production, and adopt more complex refinery configurations. Thus, the new capacity additions changed the refinery configurations from simple to deep conversion which enabled them to process low, medium, and high quality oils and biofuels.[3,4] Crude oils have a complex chemical composition and for refining industry they are characterized based on density in “light”, “medium” and “heavy” oils, degrees of quality expressed in “API gravities”, and based on oil sulfur content in “sweet” with less than 1 wt.% sulfur and “sour” crude oils when their sulfur content is higher than 1 wt.%. Some varieties of crude oils (Canada, Venezuela) contain also naphthenic acids that are very important as these acids together with the sulfur compounds represent serios corrosion challenges when such oils are processed in refineries. The types of crudes that are processed influences the yield in final products, therefore the use of “sweet” and “light” crudes is preferable, but their high prices force the refineries to use cheaper “medium” and “heavy” crude oils too in order to improve their margins.[5] However, processing heavy crudes creates economical and technical challenges as these oils are highly corrosive. The corrosive effects of heavy crude oils are mitigated and controlled in refineries by blending the low quality with higher quality oils, using corrosion inhibitors, and/or upgrading the construction materials of distilling units where possible.[6-8] All these strategies for mitigating corrosion imply further production costs therefore reducing the economic margins. Other methods like laboratory tests, corrosion models, and specific methods of optimizing the blends are largely used in the efforts to control corrosion.

Heavy crude oils processed in refineries typically have high concentrations of sulfur compounds naphthenic acids (NAP) that become extremely corrosive at the high temperatures of the distilling units. The corrosive processes generated by sulfur species and NAP acids in oil at high temperatures are very complex and as a consequence, it is generally accepted to describe them by three distinct chemical reactions.

$$Fe + 2RCOOH \rightarrow Fe(RCOO)_2 + H_2 \quad (1)$$

$$Fe + H_2S \rightarrow FeS + H_2 \quad (2)$$

$$Fe(RCOO)_2 + H_2S \leftrightharpoons FeS + 2RCOOH \quad (3)$$

NAP acids react with the metal forming iron naphthenates, a corrosion product that is oil soluble and hence being entrained constantly by the oil flow (1). The sulfur compounds in oil, especially the mercaptans and the sulfides thermally decompose generating hydrogen sulfide (H_2S) which reacts with the metal forming iron sulfide (FeS), a solid reaction product that builds up on the metal surfaces where it forms (2). The thermally generated H_2S reacts with iron naphthenates restoring the NAP and forming more FeS according to Reaction 3.[9,10] Thus, the NAP acids are reintroduced in the corrosive cycle and generate more damage to the metal. The complex mechanism of NAP acids and sulfur corrosion is very complex and insufficiently understood and known. Therefore, many research studies were dedicated to decipher the complex reaction mechanism of these two corrosive species. The present experimental work was an attempt to evaluate the effect on FeS scales of changing the oil corrosive species in sequence or order, similarly to changing the feeds in distilling towers.

EXPERIMENTAL

Experimental Procedure

The effect of running successively different crude fractions through the same apparatus was evaluated at lab scale by applying specific experimental methods and dedicated instrumentation. The experimental method that was considered appropriate for this work – the "pretreatment-challenge" - was developed to assess the integrity of the FeS scales exposed to NAP acid attack and consists of two distinct phases.[11] In the first phase FeS scales are formed at high temperatures ("pretreatment") on metal samples exposed to crude oil fractions or model compounds solutions. In the second phase, also done at high temperatures, the scales covering the samples are exposed to naphthenic acid solutions – the acidic "challenge". The corrosion rates are calculated based on samples weight losses. Separate "pretreatment" only tests were performed to evaluate the sample weight loss corresponding to this phase of the procedure. These weight losses of "pretreatment" were subtracted from initial weight of samples that were submitted to the complete experimental procedure. Thus, it becomes possible to separate and precisely evaluate the corrosive effects of each of the two experimental phases.

Similar to the "pretreatment - challenge" method, it was considered that the two crude fractions pumped successively through the same apparatus can be assimilated to the two phases described above. The first fraction, Feed 1, will form the scale (pretreatment) and the second fraction, Feed 2, will challenge the scale formed during the first phase.

Experimental Instrumentation and Materials

The "pretreatment - challenge" procedure can be done "ex-situ" when the two phases are performed in different experimental apparatuses or "in-situ" when the complete procedure is performed without interruption in the same apparatus. The present work was done in a "flow through" apparatus. The Flow Through Mini Autoclave (FTMA) allowed the experimental procedure to carrying on without interruption – "in-situ". For this experimental work simulating the "changing feeds" in oil refineries, the "pretreatment" phase was considered as "Feed 1" and the "challenge" phase as "Feed 2". Thus, in "Feed 1" a specific crude oil fraction (VGO) was pumped into reactor and in "Feed 2", a different VGO was pumped through the system.

The FTMA system presented schematically in Figure 1, has the metal samples inserted in a reactor and exposed to a constant flow of testing fluid that is supplied from different feeding tanks. The testing fluid is pumped through heated lines to the reactor which is also heated and kept to a constant high temperature during the test. The constant oil flow through the reactor ensures a constant fresh concentration of corrosive species on the sample surfaces and simultaneously removes the soluble reaction byproducts that might accumulate in the system. The oil flow rate can be controlled by the pump, and it is set to a very low value that creates flow conditions in the reactor close to those of a stagnant flow similar to those of the autoclaves. Thus, the samples are not exposed to the shear stress effects but only to the fluid corrosive species. A backpressure valve located after the FTMA reactor keeps the volatiles in the liquid during the tests preventing any gaseous phase formation. The FTMA apparatus also includes a sampling port located after the reactor fluid outlet where oil samples are collected during the tests.

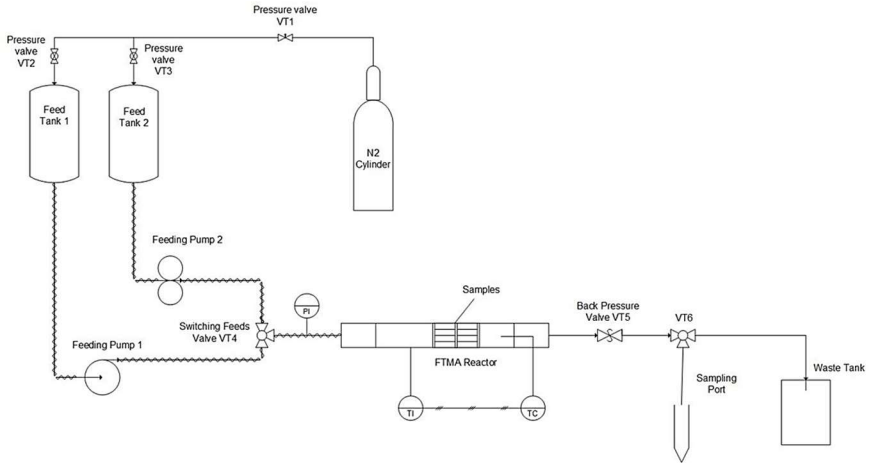

Figure 1: Schematic representation of the Flow Through Mini-Reactor (FTMA) experimental apparatus

All metal samples used in this experimental work had a rectangular shape, with geometrical dimensions of 16.2 x 15.3 mm and were made of UNS K03006 carbon steel. Four samples were used in every test, three samples for weight loss evaluations and the fourth sample for scale microscopic analysis. Before the tests, samples were polished with 400 and 600 grit silicon carbide (SiC) paper under constant isopropanol flush. After polishing the samples were cleaned and degreased with acetone, dried under nitrogen flush, their dimensions were measured precisely with a caliper, and then they were weighed on an analytical balance (initial weight). At the end of the test, samples were extracted from the reactor and the corrosion byproducts (scales) were removed mechanically and chemically from their surfaces. The superficial scale layers that formed on samples were very fragile and loose. Therefore, these scale layers were removed mechanically by brushing the samples with a stiff plastic brush under toluene flush. The strongly adherent scale that persisted on sample surfaces after the mechanical procedure were chemically removed by dipping successively the samples in Clarke solution (ASTM G 1-90).[12] Following every solution dip, the samples were dried under nitrogen flush and weighed. The sample weight at the end of the Clark solution procedure was recorded as the sample final weight and used for corrosion rate calculations.

Table 1
List of the VGO used in tests simulating the "changing feeds" in oil refineries

	Test Fluid	**TAN** (mg KOH/g oil)	**Sulfur content** (wt. %)
1	Fraction A	7.7	2.4
2	Fraction B	6.88	0.76
3	Fraction C	4.88	0.11
4	Fraction D	4.43	3.65
5	Fraction E	2.7	0.74
6	Fraction F	2.41	1.17
7	Fraction G	2.16	1.44

The experimental fluids used for this work were all crude distilling fractions – vacuum gas oils (VGO) – and they were part of a research project dedicated to NAP acid and sulfur corrosion in oil refineries. All VGO were provided from different sponsors who shared only the fractions total sulfur content (wt. %) and their total acid number (TAN) with the research group. Table 1 summarizes the total sulfur content and TAN of the selected VGO for the "changing feeds" tests.

The experimental conditions of the "changing feeds" tests are listed in Table 2.

Table 2
Experimental conditions in tests simulating the "changing feeds" in oil refineries

Test Phase	**TAN** (mg KOH/g oil)	**Sulfur content** (wt. %)	**Temp.**	**Time** (h)	**Pressure** (psig)	**Oil Flow rate** (cm^{-3}/min)
Feed 1	7.7 – 2.16	3.65 – 0.11	343ºC (650ºF)	24, 168	100	1.5
Feed 2	7.7 – 2.16	3.65 – 0.11	343ºC (650ºF)	24, 48, 168	100	1.5

The complex chemical composition and structure of the scales formed on metal surfaces were analyzed in a scanning electron microscope (JEOL JSM-6390) coupled with an energy dispersive X-ray spectrometer (EDS).

Experimental Data Processing

The corrosive effects of the VGO TAN and sulfur content were evaluated by calculating the sample corrosion rates according to the formula (1).

$$CR = \frac{(IW - FW)}{\rho_{Fe} \cdot A_s \cdot t} \cdot 24 \cdot 365 \cdot 1000 \quad (1)$$

where

CR - corrosion rate [mm/y]
IW – initial weight [kg]
FW – final weight (after last clarking) [kg]
ρ_{Fe} – Steel density [kg/m^3]
A_s – sample area exposed to corrosive fluids [m^2]
t – time of the experiment [h]

These samples weigh losses were calculated as differences between their weight measured before and after the test. As the experimental goal was to separate the corrosive effects of two different feeds processed successively, when calculating the corrosion rates for second feed, the metal weight losses measured in a separate test done with only first feed were subtracted from initial weight of the samples exposed to the complete two feeds sequence.
The scales built up on the metal surface in a multilayered structure with a complex chemical composition. The top layers of the scales were loose and fragile therefore they were easily removed from the sample surfaces during the solvent rinsing procedure. Thus, in order to quantify the scales, it was assumed that they all formed uniformly on the metal surfaces and had the same thickness in every considered point. With the superficial layers lost during sample

cleaning process it was also decided to evaluate only the strongly adherent scale layer on the samples. Based on these assumptions a theoretical adherent scale was calculated using Equation 2:

$$\delta_A = \frac{(W_{Rub} - FW)}{\rho_{FeS} \cdot A_T} \cdot 10^6 \quad (2)$$

where

δ_A – adherent scale thickness [μm]
W_{Rub} – rub weight [kg]
FW – final weight (after last clarking) [kg]
ρ_{FeS} – iron sulfide density [kg/m^3]
A_T – sample total area exposed to corrosive fluids [m^2]

In Equation 2 the W_{RUB} represents the weight of the sample after scale superficial layers were removed by mechanical means (brushing, wiping). Scale thickness is expressed in microns (μm).

RESULTS AND DISCUSSION

In oil refineries the scales, corrosion byproducts, are formed dynamically in distillation units with continuous replenishment where feeds are frequently changed and the temperatures, TAN, sulfur content, and viscosity fluctuate around operational limits. All these factors, not NAP alone, are scale damaging factors that fluctuate as the different types of crudes are distilled continuously in the unit. The scope of this work was to replicate the “changing feeds” effect on scales using a specific “flow through” apparatus, the FTMA, and different distilling fractions – VGO. Scales are the final product of sulfidation on metal surfaces which can protect against the acid corrosive effect. However, NAP acid can still reach the metal by diffusing through cracks or pores present in the scale structure. Thus, the acids not only continue to corrode the metal, but they also dissolve the scales diminishing their protective qualities and thus increasing NAP acid damaging effects. Some experimental studies published previously suggest that scales formed in NAP acid and sulfur corrosion have a more complex composition consisting both of FeS and iron oxides (Fe_3O_4 magnetite).[13,14] The presence of iron oxides in FeS scales improves their protective properties. The mechanism of iron oxide formation in NAP acid and sulfur corrosion processes is not known yet. It was hypothesized that iron naphthenates thermally decompose (Reaction 4) forming ketones and FeO (wűstite) which being unstable disproportionate to Fe_3O_4 (magnetite).

$$Fe(RCOO)_2 \rightarrow FeO + RCOR + CO_2 \quad (4)$$

All the experimental results of this work are analyzed and discussed considering this proposed mechanism of forming scales with mixed complex composition.
“Changing feeds” work used selected VGO (Table 1) that were set in different testing pairs based on their TAN, sulfur content and on volume availability. Generally, VGO with a high TAN were used in tests with VGO of a smaller TAN, as their total sulfur content was high for most of the fractions, except Fraction C which had the lowest S value (S wt.% - 0.11). The testing

variables considered for every experiment were the VGO TAN and S content and the time duration of each testing phase using a specific VGO. All other test parameters like temperature, pressure, and oil flow rate were kept constant all through the test duration. A complete summary of these “changing feeds” tests is presented in Table 3.

Table 3
Summary of the “changing feed” experiments

	Feed 1					**Feed 2**				
	Test Fluid	**TAN** (mg KOH/ g oil)	**Sulfur cont.** (wt %)	**Temp** (ºC)	**Time** (h)	**Test Fluid**	**TAN** (mg KOH/ g oil)	**Sulfur cont.** (wt %)	**Temp** (ºC)	**Time** (h)
1	Fraction B	6.88	0.76	343	24	Fraction F	2.41	1.17	343	24
2	Fraction F	2.41	1.17	343	24	Fraction B	6.88	0.76	343	24
3	Fraction A	7.7	2.4	343	24	Fraction D	4.43	3.65	343	**48**
4	Fraction D	4.43	3.65	343	24	Fraction A	7.7	2.4	343	**48**
5	Fraction E	2.7	0.74	343	24	Fraction G	2.14	1.44	343	**48**
6	Fraction G	2.14	1.44	343	24	Fraction E	2.7	0.74	343	**48**
7	Fraction B	6.88	0.76	343	**168**	Fraction C	4.88	0.11	343	**168**
8	Fraction C	4.88	0.11	343	**168**	Fraction B	6.88	0.76	343	**168**

Reference, Differential, and Total Corrosion Rates

In a complete “changing feeds” test during the first phase [of the test] the first VGO (Feed 1) reacts with the samples, corroding them and forming the scale of their surfaces. The second VGO (Feed 2) is pumped in the second phase through the reactor immediately after the first VGO and it will challenge the scales formed on samples by Feed 1. By calculating the corrosion rates corresponding to each feed (VGO) it becomes possible to evaluate the protective properties of the scales that were formed and exposed to crude fractions of different chemical composition.

The effect of Feed 1 can be easily determined by running a separate test with only that VGO (Reference Test) and measuring the metal losses later used in corrosion rates calculations. This corrosion rate is reported as the “Reference Corrosion Rate”.

For Feed 2 that follows Feed 1 in a complete “changing feeds” test, the corrosion rate can be calculated by subtracting the metal loss corresponding to Feed 1 (Reference Test) from the initial weight of samples used in the complete test. Thus, it becomes possible to separate the effect of the two different feeds and the Feed 2 corrosive effects are indicated by the “Differential Corrosion Rate”. The feeds order was also inverted for every VGO pair that was evaluated in this work. Therefore, corrosion rates were calculated also for the entire duration of a ”changing feeds” test to evaluate the feeds order effect and they were reported as “Total Corrosion Rates”. The scales thickness was calculated in a similar way to corrosion rates and it was also reported separately for Feed 1, Feed 2 and for the entire test duration – The Complete Test Scale.

The first “changing feeds” tests were using fractions B (TAN = 6.88; S = 0.76) and F (TAN = 2.41; S = 1.17) and every “feed” phase had the same duration of 24h. The complete test lasted 48h. Figure2 compares the corrosion rates for the test “B followed by F” and for the inverted

order “F followed by B” test. For the “B followed by F” sequence the scale formed with B was able to resist to the F corrosive challenge which is suggested by the lower Differential CR of F vs. the high CR of “B only”. In the inverted sequence “F followed by B”, the Differential CR of B was higher than CR of “F only” which suggests that the fraction F formed a lesser protective scale that did not hinder the corrosive species diffusion through it in the second part of the test. The Total Corrosion Rates (48h) of each of the two sequences were almost equal which indicates that the fraction order did not influence the final corrosion rates.

The scale thicknesses measured in these tests with B and F are compared in Figure 3. The scale thickness comparison suggests that in “B followed by F” test, the scale generated by F (Feed 2) was comparable to that of B (Feed 1), each of the two feeds generating similar corrosive effects. In case of the “F followed by B” sequence the scale plot (Figure 3) indicates that fraction F formed a thinner scale than B which explains why the corrosion rate of B (Feed 2) was high in this test. The thickness of the scales generated in a complete 48h test indicates a difference for the sequence order but when the scale data is compared with the CR data of same tests the results are inconsistent.

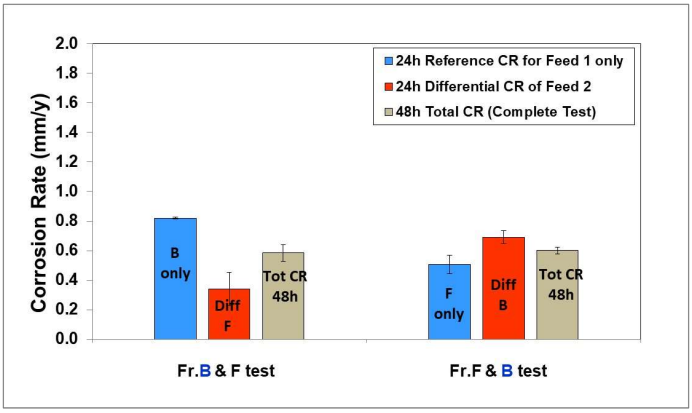

Figure 2: Corrosion rates comparison for tests using Fractions B (TAN = 6.88; S = 0.76) and F (TAN = 2.41; S = 1.17) sequence.

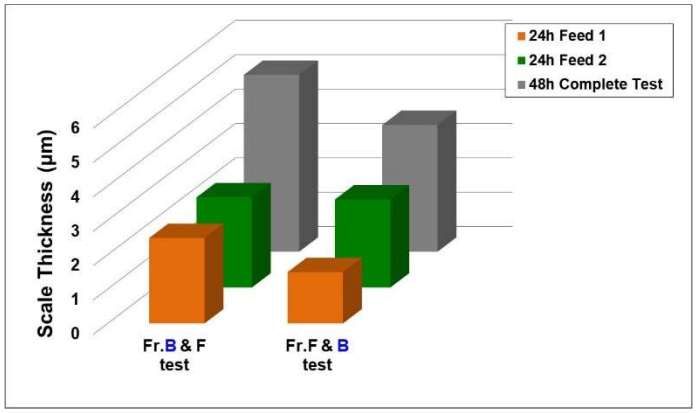

Figure 3: Scales thickness comparison for tests using the Fractions B (TAN = 6.88; S = 0.76) and F (TAN = 2.41; S = 1.17) sequence.

The results of the first “changing feeds” tests with same 48h duration (24/24), were not able to predict any difference for feeds tested in different orders. Therefore, it was decided to perform additional tests and increase the duration of the Feed 2 part to 48h. It was hypothesized that a longer exposure of the preformed scales to corrosive species of Feed 2 might show the difference between the feeds order and their effects on scale protectiveness. Two sets of VGO were selected for this part of the work, fractions A and D, and fractions E and G. All corrosion rates calculated in experiments involving these two VGO sets are presented in Figure 4. The comparison of the scales formed with the new VGO sets is presented in Figure 5.

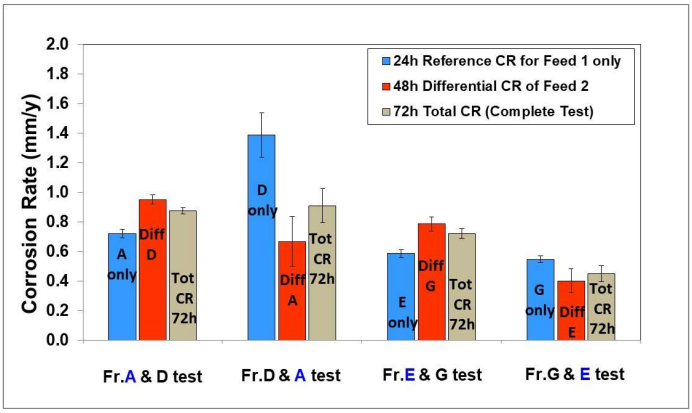

Figure 4: Corrosion rates comparison for tests using Fractions A (TAN = 7.7; S = 2.4) and D (TAN = 4.43; S = 3.65) sequence and tests using Fractions E (TAN = 2.7; S = 0.74) and G (TAN = 2.16; S = 1.44) sequence.

The comparison of Total CR in Figure 4 shows that for Fractions A (TAN = 7.7; S = 2.4) and D (TAN = 4.43; S = 3.65), the testing order of the two fractions in a successive run (24/48) had no significant effect on the final results (CR). For the same pair of VGO the Reference and Differential CR comparisons suggest that the initial scale formed by A was more protective than the similar scale formed by D. Thus, the Feed 2 challenges had different effects as it is shown by the Differential Corrosion Rates of the A and D tests.

In case of fractions E and G, a similar analysis of the Total Corrosion Rates shown in same Figure 4 suggests that this 72h corrosion rate was lower when fraction G preceded E in the sequence order than when the feeds sequence was inverted. The two fractions E and G have comparable TAN contents, but G has a higher total S content than E which might have been the key factor for the sequence order difference. The scale thickness comparisons of Figure 5 suggest that for fractions A and D tests the scale thickness was similar after 60h (complete test) regardless of the feeds order in the sequence. For fractions E and G the scale thickness results were also indicating like the CR data, the difference in the feeds order during the test. Thus, the scale thickness was smaller when fraction G preceded E than the scale formed when E preceded G.

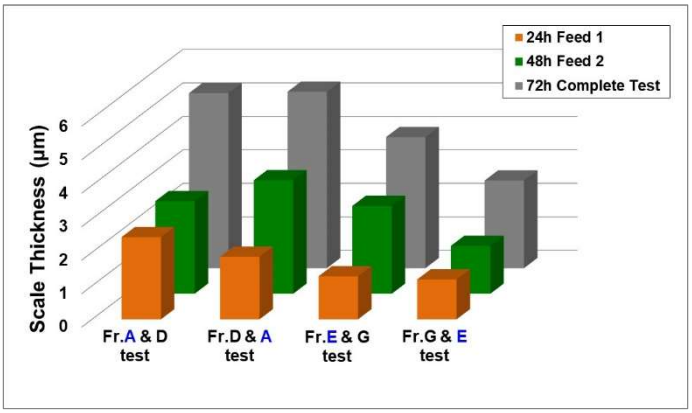

Figure 5: Scales thickness comparison for tests using Fractions A (TAN = 7.7; S = 2.4) and D (TAN = 4.43; S = 3.65) sequence and tests using fractions E (TAN = 2.7; S = 0.74) and G (TAN = 2.16; S = 1.44) sequence.

The extended time for Feed 2 in the second set of tests was able to indicate the sequence order of the feeds therefore it was decided to continue the work with two more tests when each of the two feeds is corroding the samples for 168h (7 days). Therefore, the complete test duration became 336h (14 days). The VGO selected for this long-time testing were fractions B (TAN = 6.88; S = 0.76) and C (TAN = 4.88; S = 0.11). The results of the long-time tests using fractions B and C were able to indicate that crude fractions order in a feeding sequence is decisive for the test outcome. Corrosion rates of long time tests with B and C are shown in Figure 6. Total Corrosion Rate of the “C followed by B” sequence was half of the similar corrosion rate calculated for the “B followed by C” test which clearly indicates the effect of feeds order on the test final result. Further, for the same feeds sequence the Differential CR of fraction B is almost zero which suggests that fraction B had a limited corrosive effect on the samples covered with the scales formed by C. Corrosion rates analysis for the sequence “B followed by C” suggests that scale formed by B was not very protective against the challenge of fraction C. Therefore, the calculated Differential CR of fraction C was very high. The thickness of the scales formed in the long time tests with B and C are compared in Figure 7. The plot shows that the total thickness of the scale was comparable at the end of the 336h tests regardless of the sequence order. The scale thickness calculated for each of the two feeds suggest that for the “B followed by C” sequence the fraction C (Feed 2) formed a small amount of scale when compared to fraction B (Feed 1) which might suggest that NAP acid corrosive effect was dominant for C. Corresponding corrosion rates data for this sequence (Figure 6) indicate a high corrosivity of C as Feed 2. For the sequence “C followed by B” the scale data show that despite the very low corrosion rate of B as Feed 2, the scale continued to be formed during this period of the test. Further analytical data is needed to formulate an explanation for scale growth while corrosion rate was almost zero when fraction B was used as Feed 2 in this test.

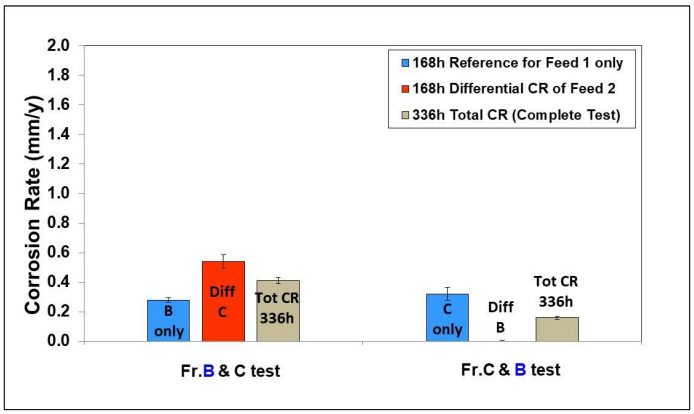

Figure 6: Corrosion rates comparison for tests using Fractions B (TAN = 6.88; S = 0.76) and C (TAN = 4.88; S = 0.11) sequence.

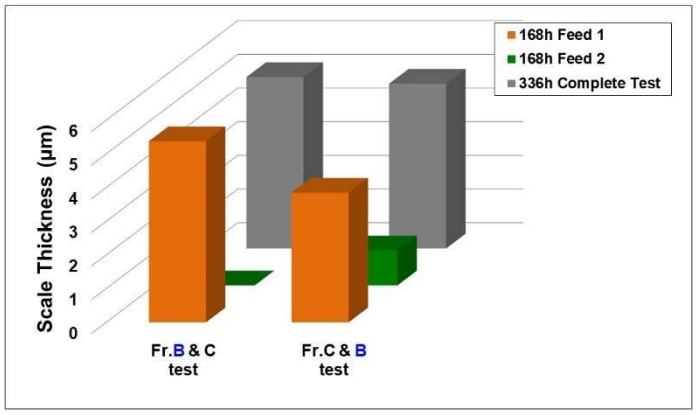

Figure 7: Scales thickness comparison for tests using Fractions B (TAN = 6.88; S = 0.76) and C (TAN = 4.88; S = 0.11) sequence.

Scale SEM/EDS Analysis

The detailed analysis of scales structure and morphology provides more information that can help in deciphering the complex mechanism of NAP acid and sulfur corrosion. Samples collected from tests of this work were embedded in epoxy resin and later they were analyzed with the SEM/EDS. The SEM analysis compares cross-sections of the scales formed in reference tests (using one Feed only) to those of scales formed in complete “changing feeds” tests (Feed 1 and 2) and these results are discussed in the following paragraphs. Figure 8 compares the cross-sections of the scale formed by fraction “B only” (a) to the scale formed by “B followed by F” test (b). Both scales are multilayered with the top layer consisting of large FeS crystals whereas the inner layers have a more dense and homogeneous structure formed of small FeS crystals. Interestingly is the inner layer configuration of the sample exposed to “B only” with a high TAN and where the acidic attack formed deep and narrow cavities into the metal that were filled by the scale. The cross-section of the “B followed by F” scale preserves the configuration formed by fraction B but it becomes thicker in 48h test. Cross-section images (c) and (d) compare the scales formed by “F only” test to the scale of “F followed by B”. Both scales of these different tests have similar configurations, but the 48h test scale (“F followed by

B") is much thicker as a consequence of the longer time exposure to fractions corrosive species. It is worth noting that scales (b) and (d) are different in structure and thickness but the final total corrosion rate of the two different tests are almost the same. It might be concluded that the scales of different morphologies are a result of the order of the two fractions in each of the two tests.

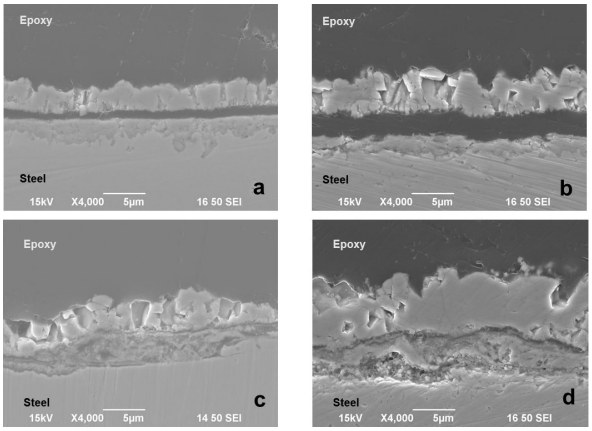

Figure 8: SEM cross-sections images of scales formed in tests using Fractions B (TAN = 6.88; S = 0.76) and F (TAN = 2.41; S = 1.17). (a) scale formed in Fraction "B only" test; (b) scale formed in "B followed by F" sequence; (c) scale formed in Fraction "F only" test; (d) scale formed in "F followed by B" sequence.

Figure 9 includes all cross-sections images for the tests using fractions A and D, images (a), (b), (c), and (d), and fractions E and G tests, images (e), (f), (g), and (h), respectively. For the A and D experiments, all SEM images show multilayered scales that became thicker when the Feed 2 duration was extended to 48h compared to 24h tests with "one feed only".

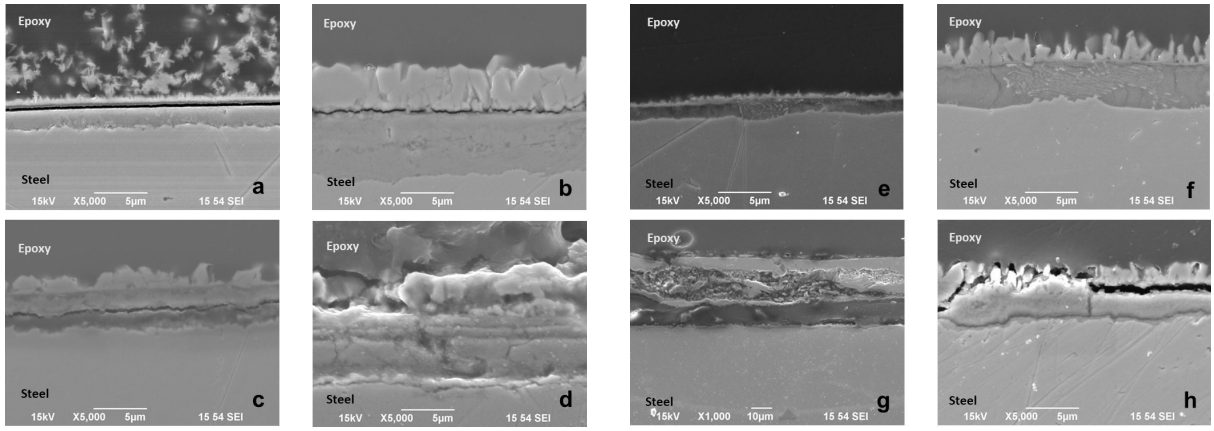

Figure 9: SEM cross-sections images of scales formed in tests using Fractions A and D (a, b, c, and d) and in tests using Fractions E and G (e, f, g, and h).
(a) scale formed by Fraction "A only"; (b) scale formed in the "A followed by D" sequence; (c) scale formed by Fraction "D only"; (d) scale formed in the "D followed by A" sequence. (e) scale formed by Fraction "E only"; (f) scale formed in the "E followed by G" sequence; (g) scale formed by Fraction "G only"; (h) scale formed in the "G followed by E" sequence.

The cross-sections images of tests with G and E suggest in fraction "E only" metal was corroded under the FeS scale leaving the cementite lamellae as "supports" of the scale top layer (Figure 9 (e)). Further, in the "E followed by G" test, both in the top and in the inner layer (Figure 9 (f))

became thicker including in the lamellae in the scale structure. The scale formed by “G only” was thick as G had double the total S content than E, therefore the cross-section image was collected at 1000X magnification (image (g)). However, when this thick scale was exposed to fraction E for 48h it became thinner (image (h)) but it still showed protective qualities as the total corrosion rate of the test was lower than the total CR of the fractions inverted order test.

Finally, for the long-time experiments of fractions B and C, the SEM analysis also included the EDS mapping analysis of the scales as the final corrosion rates indicated a clear difference for the order of the fractions sequence. Thus, the SEM images of the cross-sections showed that the scale formed by “B only” (Figure 10 (a)) was converted to a much thicker, multilayered scale, having a homogenous thick inner layer (Figure 10 (b)). The EDS mapping elemental analysis of the two scales (Figure 11) included only iron (red), sulfur (yellow) and oxygen (light blue). The EDS data for scale formed by “B only” (image (a)) shows that it consisted of a mixture of FeS and iron oxide. The scale formed in “B followed by C” was thicker but according to the EDS mapping it had a similar elemental composition of FeS and iron oxide with the two elements, O and S detected in all scale structure. The iron oxide presence in the scales is a direct result of the NAP acid thermal decomposition, a mechanism that was described and analyzed in previous published works of this group.

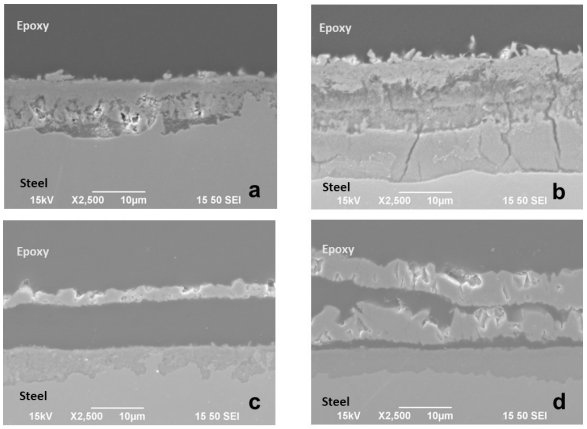

Figure 10: SEM cross-sections images of scales formed in tests using Fractions B (TAN = 6.88; S = 0.76) and C (TAN = 4.88; S = 0.11). (a) scale formed in Fraction “B only” test; (b) scale formed in “B followed by C” sequence; (c) scale formed in Fraction “C only” test; (d) scale formed “C followed by B” sequence.

Total corrosion rate of “C followed by B” test (Figure 6) suggested that Feed 2 (fraction B) had no corrosive effects on the metal covered by scale of C. However, the SEM and EDS mapping indicate that scale continued to grow under the effect of B and formed more FeS layers on the samples. The EDS elemental analysis of the scales formed in “C only” test (Figure 12 (a)) and in “C followed by B” test (Figure 12 (b)) suggests that fraction C formed a scale rich in FeS and iron oxide (image (a)) and during the “C followed by B” test (image (b)) this scale became thicker and richer in oxygen (iron oxide) and FeS. Both fractions B and C had a high TAN and as it was mentioned previously the iron oxide was formed as the effect of NAP acid thermal decomposition. The literature related to dense iron sulfide suggests that the FeS can also be oxidized to iron oxide at high temperature.[15] Thus, in these long time tests using these two high TAN fractions the scale growth can be the result of a more complex mechanism that involves not only sulfidation and acid thermal decomposition but also the FeS conversion to iron oxide.

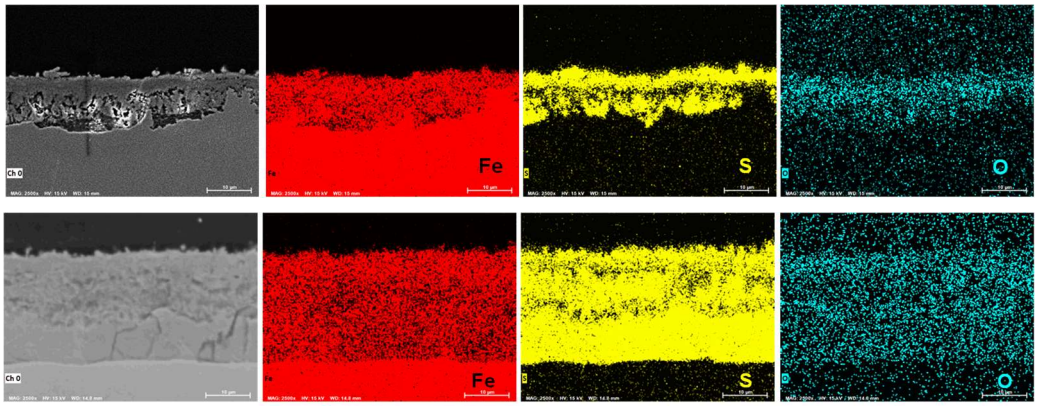

(a)

(b)

Figure 11: SEM/EDS analysis of scales formed in tests using Fractions B (TAN = 6.88; S = 0.76) and C (TAN = 4.88; S = 0.11). (a) EDS elemental mapping of scale formed in Fraction "B only" test; (b) EDS elemental mapping of scale formed in "B followed by C" sequence.

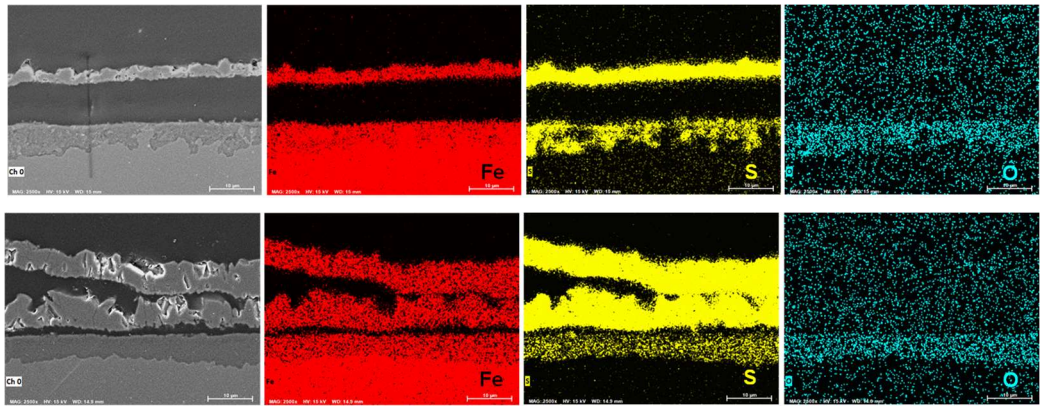

(a)

(b)

Figure 12: SEM/EDS analysis of scales formed in tests using Fractions B (TAN = 6.88; S = 0.76) and C (TAN = 4.88; S = 0.11). (a) EDS elemental mapping of scale formed in Fraction "C only" test; (b) EDS elemental mapping of scale formed in "C followed by B" sequence.

CONCLUSIONS

The effect of changing the order of two crude fractions in a testing sequence was evaluated using a specific "flow-through" apparatus and a specific testing method. Initially each of the two crude fractions was tested for the same time duration (24h) in a complete testing sequence. As the results were inconclusive the testing period for each fraction was extended until it reached 168h per fraction with the total duration of 336h for the complete test. Long time testing results made a clear distinction between different testing order of two fractions.

The SEM/EDS analysis of the scales formed in these tests indicated that scale final chemical composition depended on fractions NAP acid content (TAN) and total sulfur content. All scales consisted mainly of iron sulfide (FeS) but for particular cases (high TAN), the scales also included iron oxides formed mainly in the scale inner layer. This complex chemical structure explains the scale protective properties which was an important factor in the test results. Future work will focus on scale formation and degrading mechanism in long time testing.

ACKNOWLEDGEMENTS

The authors would like to thank to all companies that financially supported the Naphthenic Acid Corrosion Joint Industry Project (NAP JIP), the downstream research project at Ohio University and allowed them to publish the experimental results of this work.

REFERENCES

1. US. Energy Information Administration, “Short Term Energy Outlook, Global Oil Markets Forecast.” Available at: https://www.eia.gov/outlooks/steo/report/global_oil.php#:~:text=Global%20oil%20supply,million%20b%2Fd%20in%202024. (Accessed in September 2023).

2. IEA (2023), “Oil Market Report - August 2023”, IEA, Paris. Available at: https://www.iea.org/reports/oil-market-report-august-2023 (Accessed in September 2023).

3. I. Ruble; “The U.S. crude oil refining industry: recent developments, upcoming challenges and prospects for exports”, *Jour. Econ. Asymm.* 2019 (20), pp. 1-20.

4. D.K. Olsen; E.B. Ramzel; “Heavy oil refining and transportation: effect on the feasibility of increasing domestic heavy oil production”, *Fuel*, 71 (1992), pp. 1391-1401.

5. R. Kumar; R.K. Voolapali; S. Upadhyayula; “Prediction of crude oil compatibility and blend optimization for increasing heavy oil processing”, *Fuel Process. Technol*. 177 (2018), pp. 309-327.

6. S. Griffiths; B.K. Sovacool; J. Kim; M. Bazilian; J. M. Uratani; “Decarbonizing the oil refining industry: A systematic review of sociotechnical systems, technological innovations, and policy options”, *Energy Res. Soc. Sci.* 89, (2022), pp. 1-47.

7. Georgescu, O.; Constantinescu, G, Ilie, M; Georgescu, A.D.; “Anticor Type Romanian Made Corrosion Inhibitors for Refineries and Petrochemical Plant Equipment”. Mater. Corros. 2000, 51, 152-154.

8. S.D. Kapusta; A. Ooms; A.Smith; F. van den Berg; W. Fort; “Safe Processing of Acid Crudes”, CORROSION 2004, paper no. 04637, (Houston, TX: NACE, 2004).

9. Gutzeit, J.; “Naphthenic Acid Corrosion in Oil Refineries”. *Mater. Perform*. 16, (1977), pp. 24-35.

10. Piehl, R.L.; “Naphthenic Acid Corrosion in Crude Distillation Units”. *Mater. Perform.* 27 (1), (1988), pp. 37-43.

11. Wolf, H.A.; Cao, F.; Blum, S.C.; Schilowitz, A.M.; Ling, S.; McLaughlin, J.E.; Nesic, S.; Jin, P.; Bota, G.; “Method for Identifying Layers Providing Corrosion Protection in Crude Oil Fractions”. U.S. Patent 9,140,640 B2, Sep. 22, 2015.

12. ASTM G 1-90 (2011) “Standard Practice for Preparing, Cleaning, and Evaluating Corrosion Test Specimens”.(West Conshohocken, PA, Annual Book of ASTM Standards, ASTM).

13. Jin, P.; Robbins, W.; Bota, G. “Mechanism of magnetite formation in high temperature corrosion by model naphthenic acids”. *Corros. Sci.* 111 (2016), pp. 822–834.

14. Jin, P.; Bota, G.; Robbins, W.; Nesic, S.; “Analysis of oxide scales formed in the naphthenic acid corrosion of carbon steel”, *Energy Fuels*, 30 (2016), pp. 6853-6862.

15. Asaki, Z.; Matsumoto, K.; Tanabe, T.; Kondo, Y.; “Oxidation of Dense Iron Sulfide”. *Metall. Trans. B*, 14B, (1983), pp. 109-116.